CEA DAPNIA-04-188
CERN-NUFACT-Note-140

Determination of KEK 150 MeV FFAG parameters from ray-tracing in TOSCA field maps

M. Aiba[*] and **F. Méot**[†]

October 11, 2004

Abstract

Various optical parameters of the KEK 150 MeV FFAG are determined from ray-tracing in the 3-D TOSCA field maps of the radial sector triplet that constitutes a lattice cell. Two numerical integration methods are compared.

[*]KEK FFAG, Tsukuba
[†]CEA DAPNIA/SACM, Saclay

Contents

1 Introduction

The Fixed Field Alternating Gradient (FFAG) method has been proposed as a way for the acceleration of muon beams in the Neutrino Factory [1], and is now under extensive studies [2], in particular in the frame of an R&D program at KEK that has built and is operating 500 keV [3] and 150 MeV [4] proton FFAG rings.

Part of the tests to be performed on the 150 MeV proton FFAG concern, or involve a variety of machine optics configurations. Knowledge of machine optics and of its behavior is of prime importance in these studies. Considering the difficulty of modelling the optics using regular matrix or algebra methods [5], the preferred way for precision and dynamic aperture estimates is to draw machine parameters from ray-tracing in 3-D field maps.

Computation of 3-D field maps has proved to render a reliable representation of the magnets, whereas ray-tracing is probably the best mean to get accurate transport through field maps. The tracking studies are performed using usually Rung-Kutta integration [6]. Nevertheless it is considered useful to cross-check these using some other method.

This is the goal of the present work to derive machine parameters by tracking through TOSCA 3-D maps using a Taylor series based integrator [7]. An outcome are sets of large amplitude phase-space portraits including related tunes and motion stability limits, that will allow further comparison with dedicated codes.

2 Main characteristics of the 150 MeV FFAG

The 150 MeV FFAG (Fig. 1) is a 12 periods structure, each cell comprising a DFD radial sector triplet (Fig. 2) bordered by drifts of equal lengths. The main parameters of the machine and its magnet are recalled in the Table below. This study considers 10 MeV injection energy, in relation to the present injector cyclotron working conditions.

150 MeV FFAG parameters

Machine :		
energy	MeV	$12 \to 150$
geometrical radius, in/out	m	4.3 / 5.47
number of cells		12
drift size	deg	4.75
orbit extent in F magnet	m	$4.47 \to 5.20$
tune range,		
ν_r		$3.69 - 3.8$
ν_z		$1.14 - 1.3$
Magnet :		
radial triplet type		DFD
k value		7.6
max. field on orbit, F/D	T	1.63 / 0.78
RF, nominal :		
voltage, p-to-p	kV	19
frequency	MHz	$1.5 - 4.6$
harmonic		1

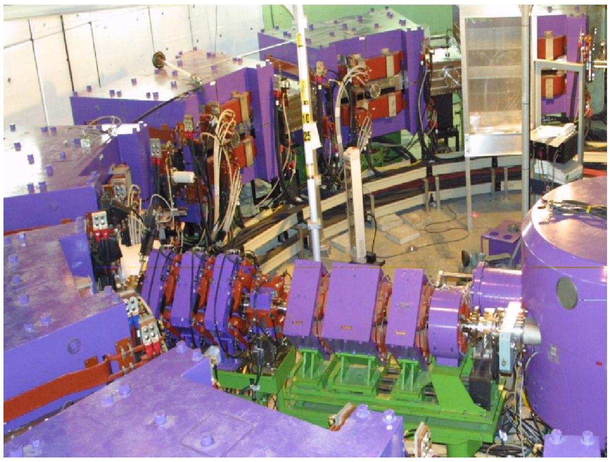

Figure 1: A view of the FFAG ring and of the injection cyclotron and 12 MeV line.

Figure 2: The 150 MeV FFAG DFD triplet. The theoretical field law in the dipoles is of the form $B(r) = B_0(r/r_0)^k$ with B_0 the field at some reference radius r_0.

3 Ray-tracing studies

Two field maps are concerned, both based on the DFD design parameters shown in Fig. 3 yielding TOSCA map geometry shown in Fig. 4. Their names as used in the following are respectively

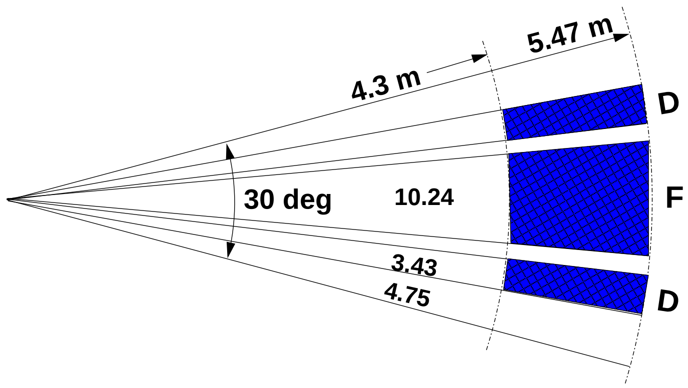

Figure 3: Geometry of the DFD sector triplet and 30 degrees sector cell.

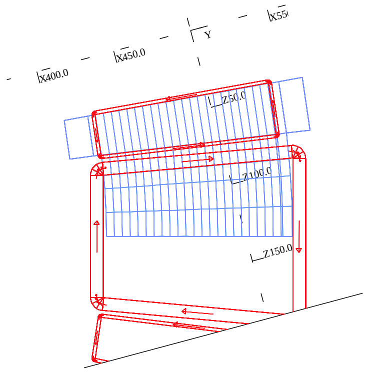

Figure 4: Geometry of TOSCA field map, covering half the angular extent.

k75v113my021f45500d3900 and k75v113my021f45500d2700. They differ by the current in the tuning coil of the D magnets of the triplet. Namely, the number of Ampère-Turns in the F coil is 45500 whereas it is respectively 3900 and 2700 in the tuning coil of the D magnets.

These tunings provide a difference in the ν_z value of the order of 0.1 (full turn) between the two designs.

The map data file itself contains a quarter of the DFD magnet, assuming symmetry firstly with respect to the median plane and secondly with respect to the vertical geometrical symmetry plane at the center of the F dipole. Developments in the ray-tracing code Zgoubi had to be performed on the one hand so as to take care of this symmetry hypothesis in making a full 3-D map from the reduced TOSCA output data, but mostly, on another hand in order for the code to be able to handle a map described in a cylindrical coordinates system - in order that what is done be clear and to allow comparison with other codes, the ingredients for that are briefly described in App. A. A typical Zgoubi data file as used in the following studies is also given in App. B, for reference.

3.1 TOSCA map k75v113my021f45500d3900

3.1.1 Sample tracking results

This Section shows sample tracking results that describe the working conditions and allow checking the correct behavior of the field reading and interpolation process.

Field data The field experienced on closed orbits (c.o. in the following) can only be known once the c.o. itself is known. Figs. 5 shows the closed orbits for 10, 22, 43, 85 and 125 MeV, determined by an iterative method : there are several manner to obtain the radius at c.o. origin, for instance by multi-turn tracking in its vicinity, in this case the center of the phase-space ellipse is the c.o. origin, or by insuring the symmetry of the trajectory or of the field experienced on that trajectory, form entrance to exit of the cell, or by insuring zero angle at cell ends. From there on the field experienced on c.o. can be obtained, it is given in Fig. 6.

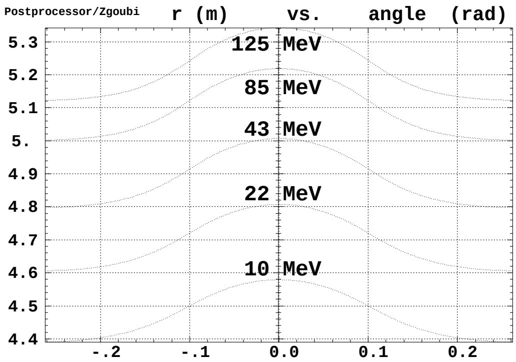

Figure 5: Closed orbits in a cell.

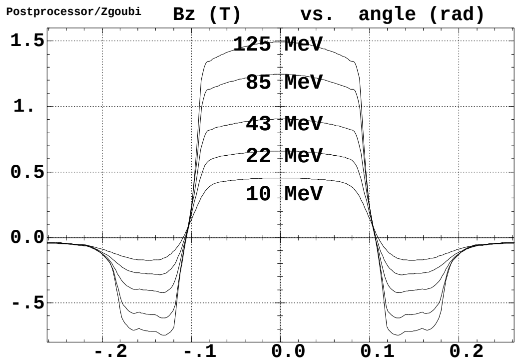

Figure 6: Field on closed orbits.

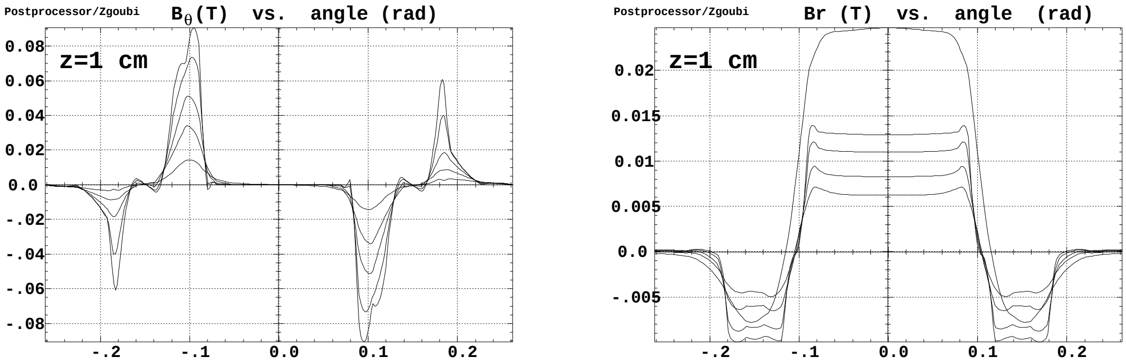

Figure 7: B_θ (left plot) and B_r (right) field components at $z = 1$ cm on parallel straight lines normal to the vertical symmetry plane of the F dipole at, respectively, $r = 4.39, 4.60, 4.79, 5, 5.12\,$m

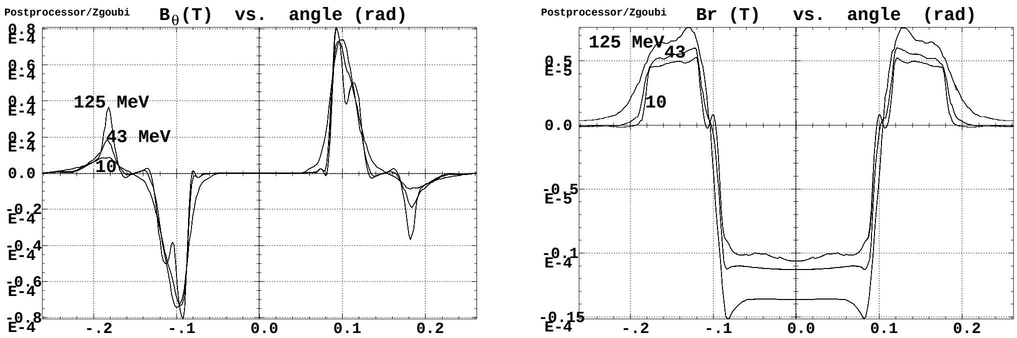

Figure 8: B_θ (left plot) and B_r (right) field components on the three vertical closed orbits of Fig. 9.

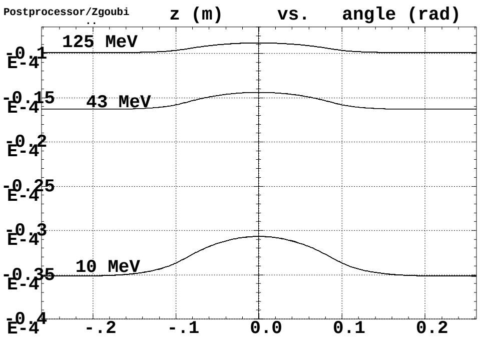

Figure 9: Residual vertical closed orbit due to non-exactly zero field in the median symmetry plane, at 10 MeV, 43 MeV and 125 MeV.

Fig. 7 checks the behavior of the magnetic field 1 cm out of the median plane. From a practical view point, this allows checking that these field values, obtained by polynomial interpolation from the 3D TOSCA data, reproduce strictly the contents of that map.

Vertical closed orbit There are mid-plane residual B_θ and B_r field components (Figs. 8) (*i.e.*, $\vec{B}$ is not exactly normal to the median plane), that come from the 3D field computation precision (since TOSCA calculations assume boundary symmetry conditions). They induce however negligible vertical closed orbit (Fig. 9), therefore they can be ignored and it is in particular not necessary to force them and their derivatives to zero for ray-tracing[1].

3.1.2 First order parameters

Tab. 1 gives the closed orbit positions, tunes (more details in Fig. 17), optical functions, etc., as a function of energy. Fig. 10 also displays the Energy-radius dependence of closed orbits as obtained from either RK4 or Zgoubi, for reference. The closed orbit is obtained by multi-turn tracking of a particle in its neighboring. The first order parameters are obtained from Twiss matrix calculation from a set of paraxial rays centered on the closed orbit. Identical results are however obtained (within their own calculation precision limit) by multi-turn tracking, ellipse matching and Fourier analysis.

In doing so, some care must be taken to get the horizontal determinant Det_r of the cell matrix close enough to one, mostly by decreasing the integration step size ; all vertical determinants on the other hand happen to differ from 1 by negligible quantity.

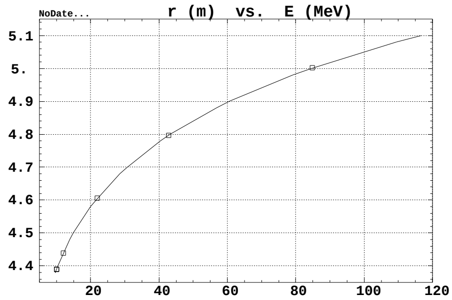

Figure 10: Radius-Energy dependence as obtained using RK4 integration (solid line) or Zgoubi (squares).

Table 1: Parameters of the cell, field map k75v113my021f45500d3900.

E (MeV)	$\frac{B\rho}{B\rho_{150}}$	$\frac{B_{Fmax}}{B_{Dmax}}{}^{(a)}$	r_{max} at drift / Fdip (cm)	$1-Det_r$	ν_r / ν_z	β_r / β_z (m)	orbit length $\mathcal{L}$ (cm)
10	0.24912	2.61	439.01 / 457.8	$2\,10^{-4}$	0.3036 / 0.1160	0.7463 / 3.9355	238.34
12	0.27304	2.54	443.97 / 463.1	$8\,10^{-6}$	0.3080 / 0.1103	0.7423 / 4.1387	241.12
21.92	0.37	2.31	460.57 / 480.6	$8\,10^{-6}$	0.3128 / 0.1165	0.7560 / 3.9979	250.27
42.82	0.52	2.13	479.70 / 500.6	$3\,10^{-5}$	0.3153 / 0.1227	0.7778 / 3.9148	260.68
84.87	0.74	2.02	500.14 / 521.8	$2\,10^{-4}$	0.3180 / 0.1167	0.8051 / 4.2441	271.72
125	0.9072	1.99	512.2 / 534.3	$3\,10^{-4}$	0.3148 / 0.1061	0.8497 / 4.747	278.15

(a) On closed orbit.

3.1.3 Large amplitude motion, vertical, 10 to 125 MeV

Fig. 11 produces a series of vertical phase-space portraits at the center of the drift, and the related horizontal phase-space motion induced by coupling, as obtained by multi-turn tracking in the k75v113my021f45500d3900 map. These show that the acceptance concerning the vertical motion is beyond the limits of the map (± 2 cm vertically with $4.47 \rightarrow 5.2$ m horizontal excursion) except for the 125 MeV region that neighbours the magnetic field homogeneity limits in the $r_0 = 5.4$ m region.

Large amplitude tunes are also indicated on the Figures for possible further comparisons with RK4 integration.

A sample Zgoubi input data file is given in App. B for reference.

[1]Note that, such may not be the case in the design stage of the FFAG triplet, where the search for Twiss parameters may require forcing $B_\theta|_{z=0}$ and $B_r|_{z=0}$ to zero in order to have exact zero vertical motion.

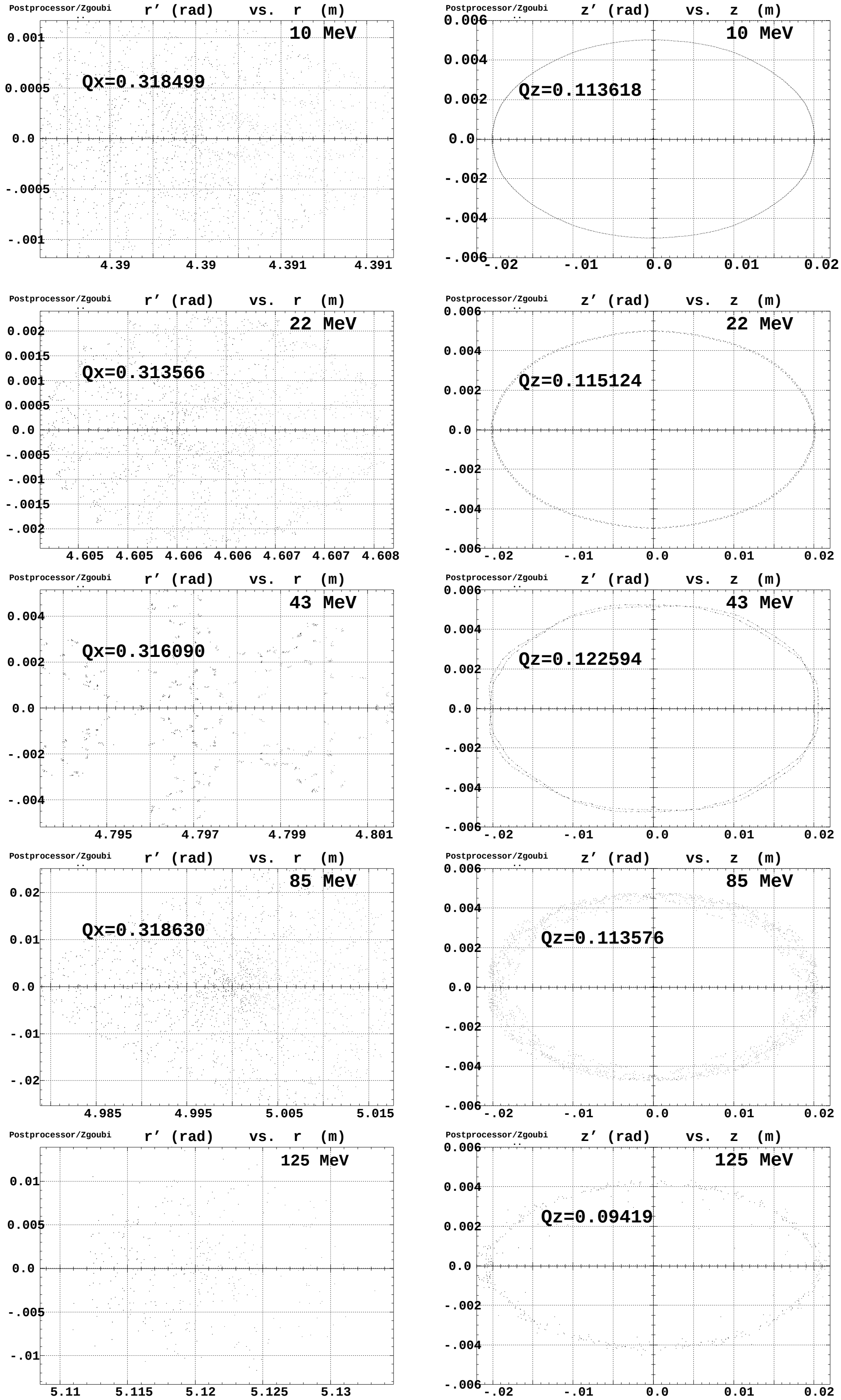

Figure 11: Right column : vertical phase-space for $z_0 = 2$ cm with $r_0 = r$(closed orbit). Left column : corresponding horizontal motion. About 2000 pass in a cell. Cell-tune values shown are obtained by Fourier analysis ; the paraxial tunes (not shown) are given in Table 1. Note : the 125 MeV, $z_0 = 2$ cm particle only survives about 500 periods.

3.2 TOSCA map k75v113my021f45500d2700

3.2.1 Sample tracking results

The closed orbits and field on c.o. do not differ sensibly from the 3900 A.T case (Figs. 5, 6), as can be seen in Figs. 12, 13.

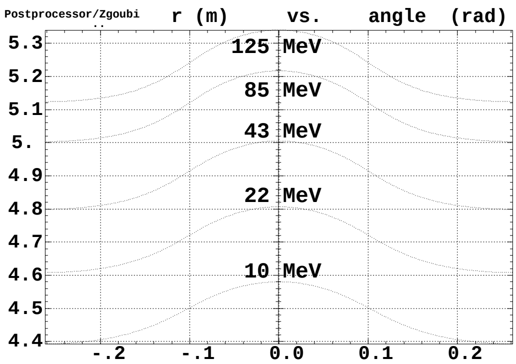

Figure 12: Closed orbits in a cell.

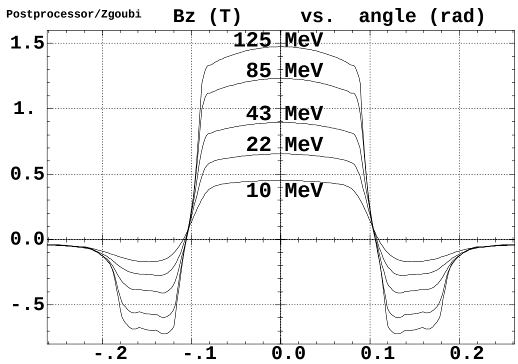

Figure 13: Field on closed orbits.

3.2.2 First order parameters

The Table below gives the closed orbit positions, tunes optical functions, etc. as a function of energy. These quantities have been obtained as described in Section 3.1.2 (p. 6).

Table 2: Parameters of the cell, field map k75v113my021f45500d2700.

E (MeV)	$\frac{B\rho}{B\rho_{150}}$	$\frac{B_{F_{max}}}{B_{D_{max}}}^{(a)}$	r_{max} at drift / Fdip (cm)	$1 - Det_r$	ν_r / ν_z	β_r / β_z (m)	orbit length $\mathcal{L}$ (cm)
10	0.24912	2.66	439.2 / 457.9	$2\,10^{-5}$	0.3036 / 0.1050	0.7508 / 4.3324	238.370
12	0.27304	2.60	444.1 / 463.2	10^{-5}	0.3071 / 0.1001	0.7494 / 4.5487	241.120
21.92	0.37	2.36	460.7 / 480.6	$3\,10^{-5}$	0.3111 / 0.1067	0.7664 / 4.3578	250.208
42.82	0.52	2.18	479.8 / 500.5	$5\,10^{-5}$	0.3132 / 0.1126	0.7911 / 4.2573	260.576
84.87	0.74	2.06	500.2 / 521.6	610^{-5}	0.3157 / 0.1055	0.8185 / 4.6920	271.581
125	0.9072	2.04	512.3 / 533.9	$4\,10^{-4}$	0.3130 / 0.0951	0.8601 / 5.2888	277.984

(a) On closed orbit.

3.2.3 Large amplitude motion, 10 to 125 MeV

Fig. 14 produces a series of horizontal phase-space portraits at the center of the drift and related tunes, as obtained by multi-turn tracking in the k75v113my021f45500d2700 map. The triangular shape of the large amplitude motion is induced by the large sextupole component[2] in $B(r)$. The limits in the horizontal motion are addressed below. Large amplitude tunes are again indicated on the Figures for possible further comparisons with RK4 integration.

Note that as in the k75v113my021f45500d3900 map case, in the 125 MeV region the motion is restrained in amplitude due to the field map homogeneity limits in the $r_0 = 5.4$ m region.

Fig. 14 produces a series of vertical phase-space portraits at the center of the drift. The same remark of field map limits holds as to the 125 MeV case.

[2]In 150 MeV FFAG the horizontal dynamic aperture is determined by structural (12 periods) sextupole. Horizontal tune is selected not to be too close to $\nu_r = 4$ to keep enough acceptance. Generally, if horizontal tune per cell is close to 1/4 or 1/5, then amplitude limit is determined by octupole or decapole.

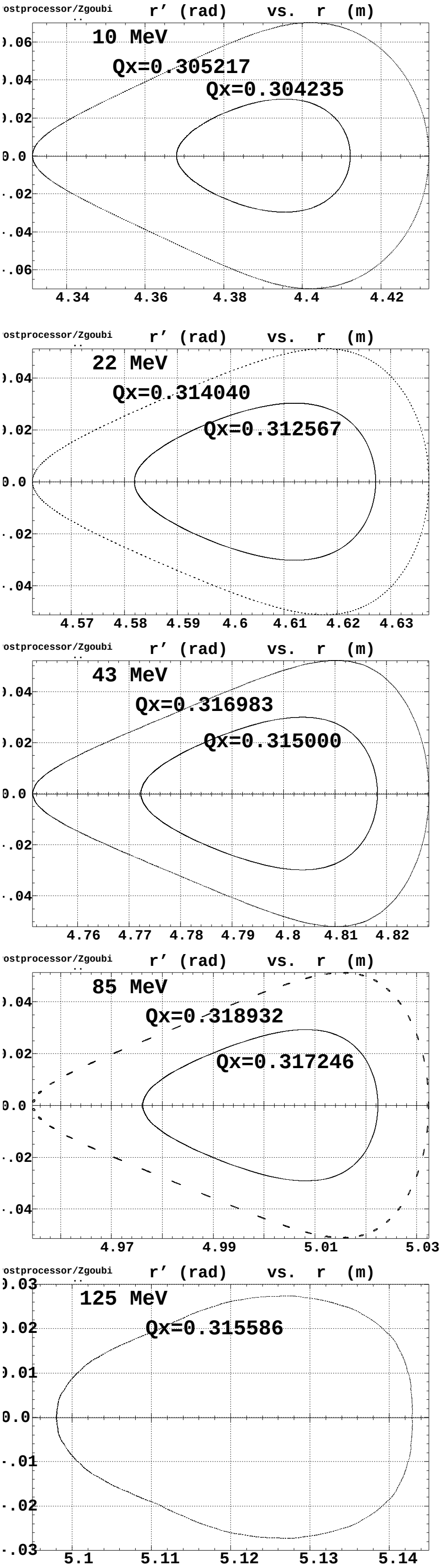

Figure 14: Horizontal motion. Tunes are from Fourier analysis. The inner motion is 3500 pass in a cell the outer one is 4700.

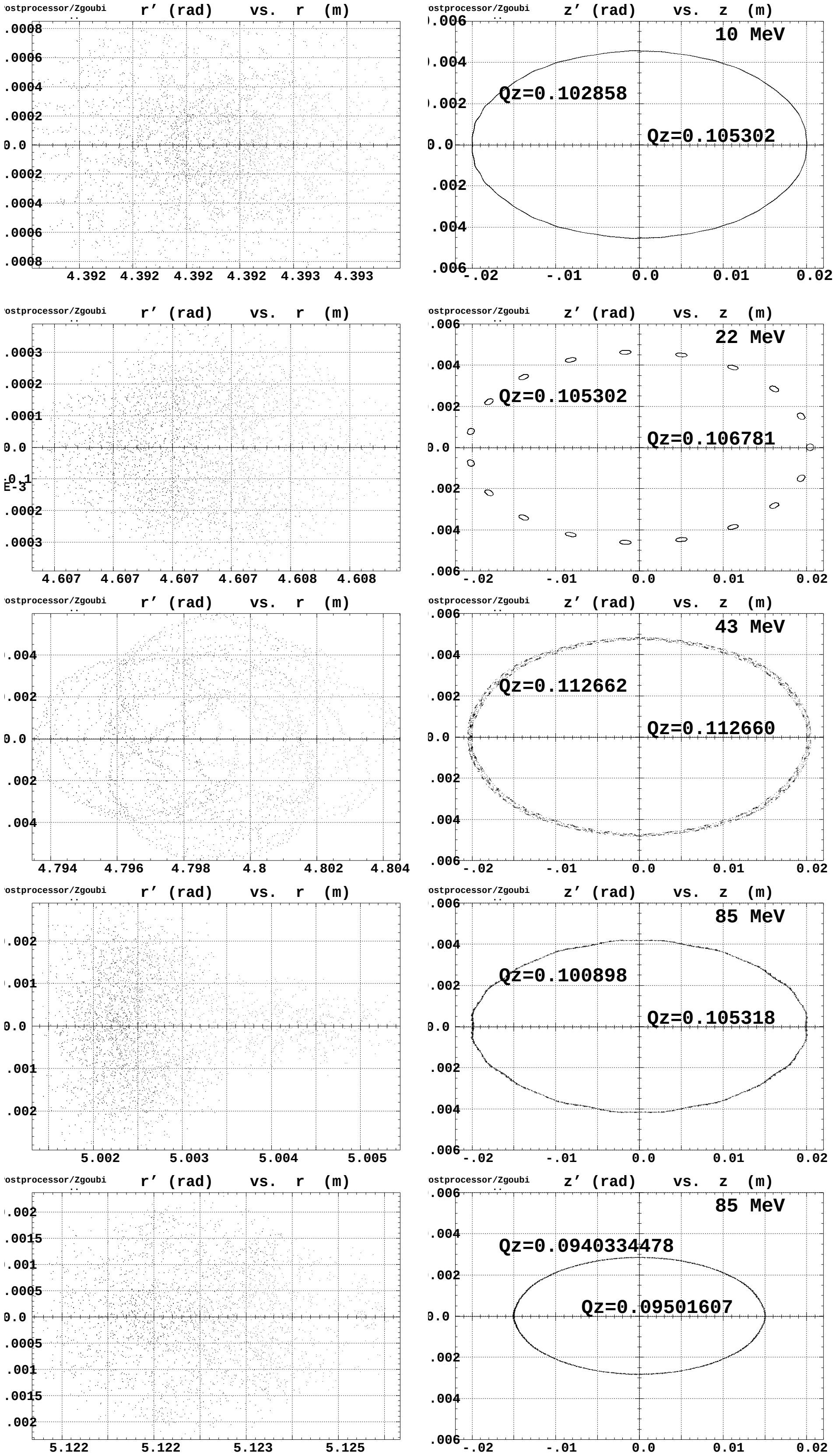

Figure 15: Right column : vertical phase-space for $z_0 = 2$ cm with $r_0 = r_{closed\ orbit}$ ($z_0 = 1$ cm for 125 MeV). Left column : corresponding horizontal motion. 3200 periods.

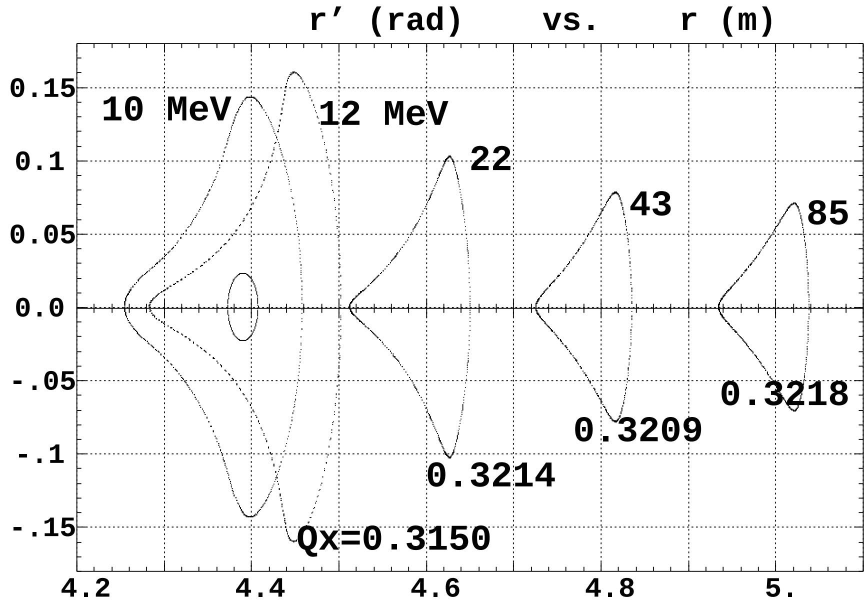

Figure 16: Stability limits at various energies (about 10^3 machine turns). The ellipse within the 10 MeV stability on the left represents the nominal $\epsilon_r = 0.04$ πcm beam at injection. Cell tunes are given.

Horizontal acceptance Horizontal amplitude is pushed further in Fig. 16 that shows the limits of stable motion for 5 energies, with better than $\Delta r = \pm 0.1$ mm accuracy. The corresponding geometrical acceptance given this particular optical tuning can be estimated using $A_r \approx H \times B/2$ with H the height and B the base of the more or less triangular figure ; so obtained A_r values are given in the Table aside.

The small ellipse within the leftmost stability domain in Fig. 16 represents for illustration an $\epsilon_r = 0.04$ πcm invariant centered on the local closed orbit (10 MeV, $r = 4.39$ m).

Horizontal acceptance.

E (MeV)	r_{co} (m)	$H \times B \,/\, 2\pi$ (cm)	$\beta\gamma A_r/\pi$ (cm)
10	4.390	0.92	0.14
12	4.440	1.12	0.18
21.92	4.606	0.45	0.10
42.82	4.797	0.27	0.08
84.87	5.001	0.23	0.10

Such precise description of the motion near to or on a separatrix as shown in Fig. 16 requires a high degree of symplecticity of the numerical integrator (a feature already demonstrated earlier for non-linear dynamic studies, cf. for instance 6-D simulation of resonant extraction Ref. [8], 6-D dynamic aperture in rings Ref. [9]). In particular getting these curves takes a very large number of turns (thousands) if the fractional tune gets very close to $1/3$; in spite of this the phase-space portraits show no such effects as spreading or spiral motion.

4 Comments

One goal of these tracking simulations was to derive machine tunes in two different cases of F/D magnetic field ratio in the DFD triplet. Tunes computed using Zgoubi (Tabs. 1, 2) have been compared to Runge-Kutta results, the agreement is excellent as shown in Fig. 17. The difference in tunes between the two optics is summarized in the Table below.

Theoretical interpretation of the results obtained is succinct, given the purpose of the study, yet the point

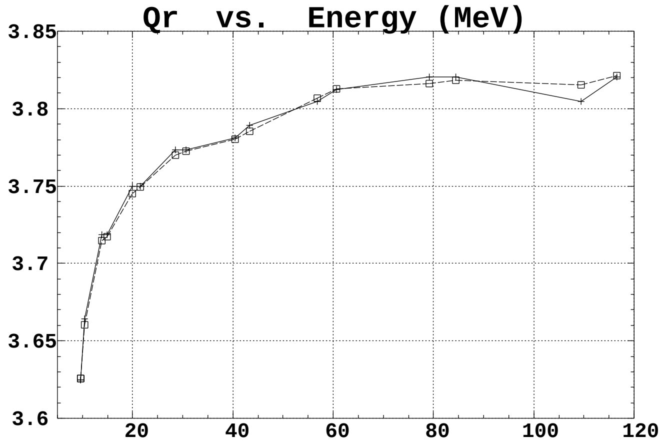

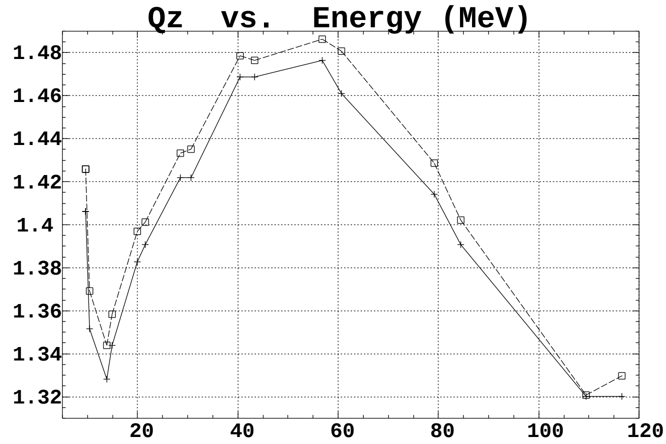

Figure 17: Radial tune (left plot) and axial tune (right) as a function of energy, as obtained using RK4 integration (solid lines/crosses) and using Zgoubi (dashed line/squares).

is addressed in more detail in another paper, Ref. [10], in which the these field map based tracking results are compared with a 3-D geometrical simulation of the FFAG magnets.

Another goal was to test the efficiency of the computation of large amplitude motion, and produce sample large amplitude tune values. Results show that Zgoubi fairly preserves the basic motion invariants even in separatrices regions. An interesting consequence of that feature is that it confirms the code as an efficient tool for dynamic aperture as well as for amplitude and momentum detuning estimates.

An outcome of the studies is in CPU time consumption. The Taylor series based method appears to be fast, at a high degree of accuracy on motion computation.

E (MeV)	$\Delta\nu_r$ / $\Delta\nu_z$ (3900A→2700A) full turn
10	0 / 0.1320
12	0.0108 / 0.1224
21.92	0.0204 / 0.1176
42.82	0.0252 / 0.1212
84.87	0.0276 / 0.1344
125	0.0216 / 0.1320

Acknowledgements

One of us (FM) thanks Pr. Y. Mori for offering the possibility of a stay at KEK, in Aug. 2004, in order to collaborate to these studies on the 150 MeV FFAG ring.

Franck Lemuet is acknowledged for his providing various Zgoubi data and rereading the manuscript.

APPENDIX

A 3-D field map in cylindrical coordinates

So far Zgoubi could only handle 3-D maps defined in Cartesian mesh [7, Users' guide, Sec. 1.4.4]. A second degree interpolation is used based on the polynomial

$$B_l(X,Y,Z) = A_{000} + A_{100}X + A_{010}Y + A_{001}Z + A_{200}X^2 + A_{020}Y^2 + A_{002}Z^2 + A_{110}XY + A_{101}XZ + A_{011}YZ$$

with B_l standing for any of the three components B_X, B_Y, or B_Z and with X, Y, Z being the distance from particle position to the center of a nearest $3 \times 3 \times 3$ points interpolation parallelepipedic volume.

In the present case of cylindrical coordinates with axis in the Z direction, angle θ and radius r measured from the center of the FFAG, the same formalism is used without any change by simply considering that $X = \theta$ and $Y = r$.

The calculation of the polynomial coefficients needs however be followed by a transformation from the (r, θ, Z) map frame to the (x, y, z) Cartesian frame of trajectory calculation, of the form (after Ref. [7, Users' guide, Sec. 1.4.2]) $\frac{\partial B}{\partial x} = \frac{1}{r}\frac{\partial B}{\partial \theta}$, $\frac{\partial B}{\partial y} = \frac{\partial B}{\partial r}$, $\frac{\partial^2 B}{\partial x^2} = \frac{1}{r^2}\frac{\partial^2 B}{\partial \theta^2} + \frac{1}{r}\frac{\partial B}{\partial r}$, etc.

B Zgoubi data file

```
  'OBJET'
 502.1500879                        Rigidity - kG.cm   (12MeV proton)
 2
1    1
447.8666    0.    1.     0. 0.  1.   'o'
1
 'PARTICUL'
938.2723 1.60217733D-19 0. 0. 0.
'FAISTORE'                          ''Pick-up'' - store output data for graphic/analysis
  b_zgoubi.fai #START
1
 'SCALING'    #START                RF frequency law
   1   1
CAVITE
2    12MeV        150MeV
     1.        2.75527584
     1          21236
  'TOSCA'                           TOSCA field map, 1 cell
   0  0
  -1.e-3   1. 1. 1.                 So as to get B-kG, angle-rad, radius-cm, z-cm
  FFAG 150MeV
  301 121 41   20                   Mesh data : IX(angle) JY(radius) KZ  MOD(symmetrization)
b_k75v113my021f45500d3900.table
  0 0 0 0
  2
 .1                                 Integration step size (cm)
  2
 0. 0. 0. 0.
-----------  repeat TOSCA cell -----------
-----------     11 times       -----------
  'CAVITE'                          Accelerating cavity
   6
  1.619864859720890e6   12.         f0 (Hz),  starting synchronous Ekin W_s0 (MeV)
  19000.  0.3490658504              Vp (V),  phi_s (rad)
'REBELOTE'                          Multiturn tracking (21236 turns)
21235 0.1 99
'END'
```

References

[1] A Feasibility Study of A Neutrino Factory in Japan, NufactJ Working Group, KEK, May 24, 2001.

[2] See for instance http://hadron.kek.jp/FFAG/FFAG04_HP/index.html, http://www.triumf.ca/ffag2004/.

[3] http://hadron.kek.jp/FFAG/photo/index-pop.html.

[4] Commissioning of 150MeV FFAG Synchronisation, Y. Yonemura et *als.*, EPAC2004.

[5] Beam optics and dynamics of FFAG accelerators, S. Machida and E. Forest, CP600, 16th Int. Conf. Cyclotrons (2001).

[6] Beam dynamics of FFAG accelerator, M. Aiba, ICFA-HB2002.

[7] The ray-tracing code Zgoubi, F. Méot, NIM A 427 (1999) 353-356, and also for details, Zgoubi users' guide - Version 4, F. Méot and S. Valero, Reports FERMILAB-TM-2010 / CEA DAPNIA-97-13 (1997).

[8] Hadrontherapy project ETOILE, Reconstruction of the slowly extracted beam, F. Méot, report CEA DSM DAPNIA-02-176 (2002).

[9] On fringe field effects in the FERMILAB 50 GeV muon storage ring, C. Johnstone, F. Méot, Proc. PAC2001 Conf. ; Dynamic aperture studies in the FERMILAB proton driver, F. Méot, C. Johnstone, A. Drozhdin, report CEA DAPNIA/SEA-01-05 (May 2001).

[10] Developments in the ray-tracing code Zgoubi for multiturn tracking in FFAG rings, F. Méot and F. Lemuet, CEA DAPNIA-04-278 (2004), to be published.